RESEARCH ARTICLE

DEVELOPMENT

Identification of a regeneration-organizing cell in the *Xenopus* tail

C. Aztekin[1,2]*, T. W. Hiscock[1,3]*, J. C. Marioni[3,4,5], J. B. Gurdon[1,2], B. D. Simons[1,6,7]†, J. Jullien[1,2]†

Unlike mammals, *Xenopus laevis* tadpoles have a high regenerative potential. To characterize this regenerative response, we performed single-cell RNA sequencing after tail amputation. By comparing naturally occurring regeneration-competent and -incompetent tadpoles, we identified a previously unrecognized cell type, which we term the regeneration-organizing cell (ROC). ROCs are present in the epidermis during normal tail development and specifically relocalize to the amputation plane of regeneration-competent tadpoles, forming the wound epidermis. Genetic ablation or manual removal of ROCs blocks regeneration, whereas transplantation of ROC-containing grafts induces ectopic outgrowths in early embryos. Transcriptional profiling revealed that ROCs secrete ligands associated with key regenerative pathways, signaling to progenitors to reconstitute lost tissue. These findings reveal the cellular mechanism through which ROCs form the wound epidermis and ensure successful regeneration.

Appendage regeneration requires coordinated changes in many cell types and has largely been characterized by morphological assessments, lineage-tracing studies, and low-throughput gene investigations. As a result, regeneration is broadly divided into three essential steps: the formation of a specialized wound epidermis, blastema or regenerative bud formation, and outgrowth via proliferation (*1*, *2*). However, a comprehensive understanding of the changes in cell types, transcriptional dynamics, and cellular mechanisms accompanying these processes is lacking. For example, the first morphological change after amputation is the formation of the specialized wound epidermis, a ligand-expressing structure covering the wound that is essential in many regeneration scenarios in different species (e.g., zebrafish, axolotl) (*1*, *3*, *4*). It is not clear which cell types are present in the specialized wound epidermis, what its origin is, what ligands are expressed from it, or why it is crucial for regeneration. To answer such questions and identify essential regulators of regeneration, we focused on *Xenopus* tadpoles, which, with their naturally occurring regeneration-competent and -incompetent developmental stages, are an ideal model for comparative studies (*5*).

[1]Wellcome Trust/Cancer Research UK Gurdon Institute, University of Cambridge, Cambridge, UK. [2]Department of Zoology, University of Cambridge, Cambridge, UK. [3]Cancer Research UK Cambridge Institute, University of Cambridge, Cambridge, UK. [4]EMBL–European Bioinformatics Institute, Wellcome Genome Campus, Cambridge, UK. [5]Wellcome Sanger Institute, Wellcome Genome Campus, Cambridge, UK. [6]Department of Applied Mathematics and Theoretical Physics, Centre for Mathematical Sciences, University of Cambridge, Cambridge, UK. [7]Wellcome Trust Centre for Stem Cell Research, University of Cambridge, Cambridge, UK.
*These authors contributed equally to this work.
†Corresponding author. Email: jj256@gurdon.cam.ac.uk (J.J.); bds10@cam.ac.uk (B.D.S.)

Single-cell transcriptomics reveals developmental, amputation-related, and regeneration-specific changes

To assess comprehensively the transcriptional dynamics and cell-type changes that occur during regeneration, we used high-throughput single-cell RNA sequencing (scRNA-seq) to analyze *Xenopus laevis* tails at various stages after amputation in both regeneration-competent and -incompetent tadpoles, as well as uninjured (intact) tails at the same developmental stage (Fig. 1A). We sequenced >13,000 cells, with at least two biological replicates per condition, with an average of ~2300 genes detected per cell (table S1). Cells from all samples were pooled and visualized by the dimensionality reduction method UMAP (*6*) (Fig. 1A). Cluster identity was assigned using multiple known markers and revealed 46 putative cell types (some rare and others uncharacterized) encompassing the immune system, skin, nervous system, and somites, thus emphasizing the cellular heterogeneity of the tail (Fig. 1B and fig. S1). Biological replicates showed a similar distribution of cell types, confirming the reproducibility of the atlas (fig. S2). Computational inference of cell cycle state indicated that progenitor cell populations are mostly positioned in G_2/M and S phases, whereas terminally differentiated cells are in G_1 (fig. S3). Our comprehensive cell atlas can be viewed using an interactive platform (marionilab.cruk.cam.ac.uk/XenopusRegeneration/).

Having established the atlas, we then assessed what transcriptional and cell-type changes are associated specifically with tail regeneration. By comparing samples, we could make a distinction between developmental (Fig. 2A), amputation-specific (Fig. 2B), and regeneration-specific (Fig. 2C) effects. Most cell types were found in all samples (fig. S4A). We found no evidence for the emergence of a multipotent progenitor population during regeneration, nor did we observe intermediate cell states reflective of transdifferentiation, results which are consistent with those of lineage-tracing studies (*7*). Indeed, the only previously unknown cell type to emerge after amputation was an uncharacterized motor neuron–like cell type that expressed genes associated with spinal cord injury (e.g., *Fgf10*) (*8*) and metabolic hormones (e.g., *Leptin*) (*9*, *10*) (Fig. 2B). This phenotype was also observed in regeneration-incompetent tadpoles (Fig. 2B). Therefore, we considered it an amputation response and focused instead on regeneration-specific changes.

Surveying the range of single-cell data, we found that the most significant cell-type change specific to regeneration was related to a previously unidentified cell type of the epidermis (fig. S4), which we designated as the regeneration-organizing cell (ROC). On the basis of the scRNA-seq data, ROCs were found in both intact and regenerating tails but were observed after tail amputation only in regeneration-competent tadpoles (Fig. 2C). As this cell population distinguishes the amputation response of regeneration-competent tadpoles from regeneration-incompetent ones and expresses multiple genes that support regeneration [e.g., *Wnt5a* (*11*), *Fgf10* (*12*), *Fgf20* (*13*), and *Msx1* and *Bmpr1a* (*5*)], we hypothesized that ROCs may represent an essential component of the regenerative response.

Relocalization of ROCs forms the specialized wound epidermis

To assess the function of ROCs, we first investigated their location using marker genes identified by scRNA-seq. Using published in situ data from Xenbase, we found that >25 ROC marker genes were expressed along the midline edge of the epidermis (e.g., *Fgf7*, *Msx2*, *C3*, *Wnt3a*), from the posterior trunk toward the tail tip (table S2). We further confirmed the localization of ROCs using a *Lef1* reporter line [pbin7Lef:GFP (GFP, green fluorescent protein)] (*14*) in combination with TP63 immunolabeling. Although *Lef1* is expressed in multiple cell types, only ROCs express high levels of both *Lef1* and *Tp63* (Fig. 3A and fig. S5A). Therefore, we identified ROCs as LEF1+/TP63+ cells and confirmed that they are localized to the edge of the epidermis (Fig. 3B and fig. S5B). ROCs are present in this location in both regeneration-competent and -incompetent tadpoles, and immediately after amputation, this population is largely removed from the amputation plane but remains along the posterior trunk (Fig. 3C, left-hand column). During successful regeneration, ROCs reappear in the amputation plane within 24 hours; however, they remain notably absent at the amputation plane of regeneration-incompetent tadpoles (Fig. 3, C and D, and fig. S5C). Our *Lef1* data were consistent with published in situ data of ROC marker genes seen in the tails of amputated regeneration-competent tadpoles

[*Fgf9*, *Fgf10*, *Wnt5a*, *Wnt3a*, *Msx1*, *Msx2* (*5*, *15*); *C3* (*16*)] and lacking in regeneration-incompetent tadpoles [*Msx1* and *Msx2* (*5*, *15*)]. The gene expression profile and location of ROCs at the amputation plane suggest that ROCs are in fact a single cell type that defines the specialized wound epidermis, which specifically forms in regeneration-competent tadpoles to trigger the regenerative response.

As the presence of ROCs at the amputation plane correlates with regenerative outcome, we tested whether these cells are required for regeneration. We first performed nitroreductase/metronidazole–based genetic ablation (*17*) of ROCs using F_0-transgenic tadpoles expressing nitroreductase (NTR) under the control of the *Krt.L* promoter (*Krt.L* is also known as *Krt70.L*), a member of the keratin gene family that is expressed in a highly specific manner in ROCs in stages where regeneration is assessed (Fig. 4A and fig. S6, A to D). After metronidazole (MTZ) treatment, we were able to specifically ablate ROCs, as confirmed by the disappearance of GFP-positive cells in pbin7Lef:GFP/Krt.L:NTR F_0 transgenic tadpoles (Fig. 4A), together with the observation of no apparent gross off-target effects in other tissue types (fig. S6E). Ablation of ROCs in regeneration-competent tadpoles led to drastically reduced tail regeneration (Fig. 4B and fig. S7, A to D), demonstrating that ROCs are indeed required for regeneration.

We then eliminated ROCs in a spatially localized manner, by manually removing ROCs in the posterior trunk that remain directly after amputation (Fig. 4C and fig. S7E). When these regions were removed at the same time as the amputation, we observed a reduction in *Lef1*+ cells at the amputation plane and correspondingly reduced regeneration (Fig. 4D and fig. S7E). However, when these regions were removed 12 to 16 hours after amputation, *Lef1*+ expression was maintained at the amputation plane, and regeneration could proceed (Fig. 4, C and D, and fig. S7E), indicating that there is a critical time window during which posterior trunk ROCs are required to initiate regeneration. This suggests that, soon after amputation, existing ROCs may have to relocate to the amputation plane to initiate the regenerative response. To test this hypothesis, we traced ROCs with the *Lef1* reporter and observed the mobilization of resident ROCs from the posterior trunk toward the amputation plane within 2 to 8 hours after amputation (Fig. 4E). Together, these observations suggest that mobilization of ROCs to the amputation plane is a necessary step in wound epidermis formation and subsequent regeneration, which contrasts with previous suggestions that the wound epidermis is a distinct state that differs from normal epithelium and appears after amputation (*2*).

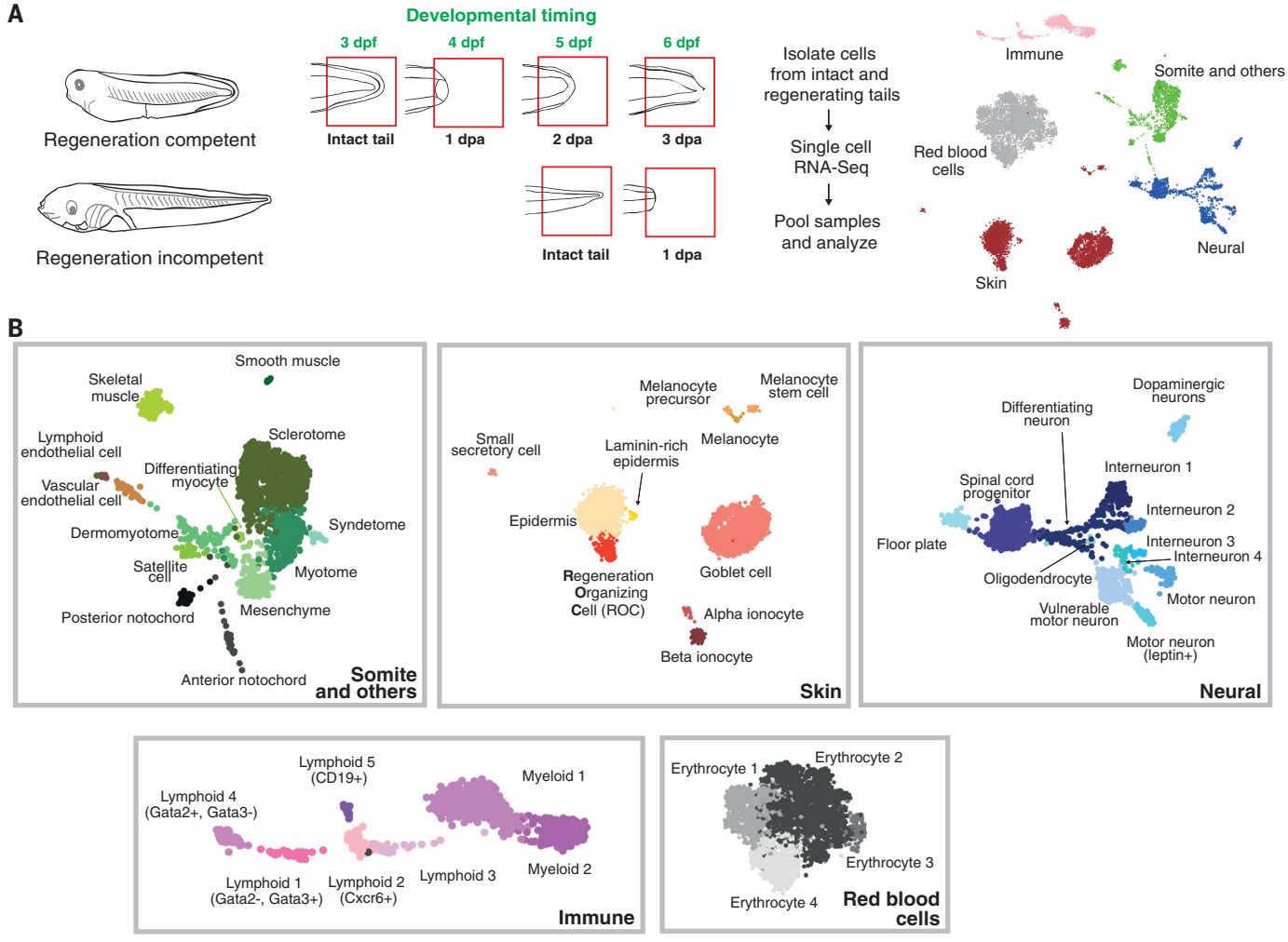

Fig. 1. Pooled transcriptional cell state atlas of the *Xenopus laevis* tail before and after amputation. (**A**) Samples were prepared for single-cell RNA-seq analysis from regeneration-competent and -incompetent tadpoles by collecting either intact tails or tails at various stages after amputation: 1 to 3 days postamputation (dpa) for regeneration-competent, and 1 dpa for regeneration-incompetent tadpoles. Developmental timing is indicated for each sample (days postfertilization, dpf). (Right) Samples were processed separately for sequencing, with at least two biological replicates per condition, and then pooled for UMAP visualization (see supplementary materials and methods). Each dot represents a single cell; color indicates main tissue group. (**B**) Cluster identities based on established cell-type markers. For details of cluster annotations, see main text, fig. S1, and supplementary materials and methods.

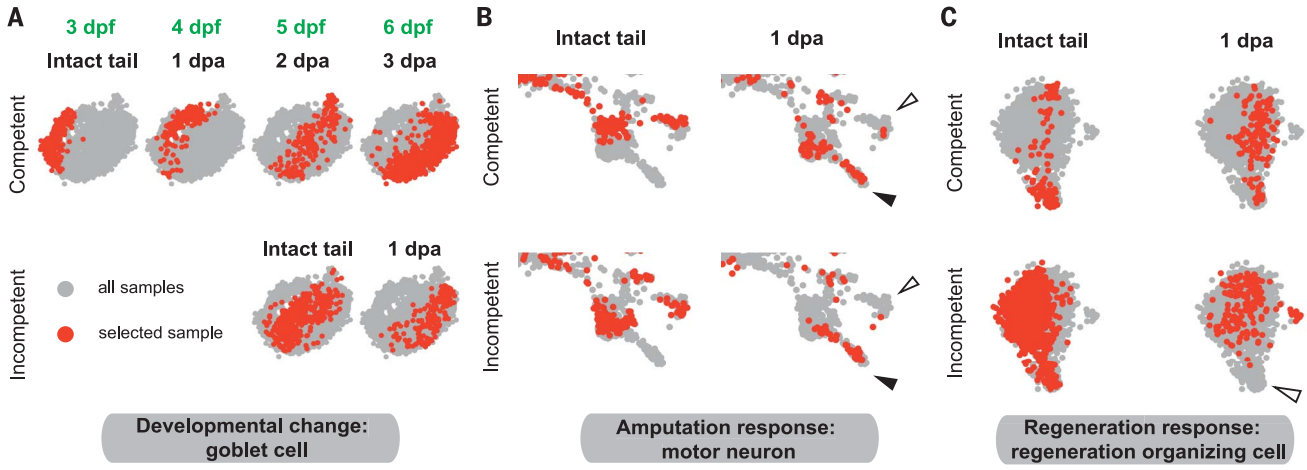

Fig. 2. Comparison of scRNA-seq samples discriminate gene expression and cell state changes that take place during development from those associated with the response to amputation or regeneration. Examples of cell-specific gene expression changes that take place (A) during development, (B) in response to amputation, and (C) in response to regeneration. Gray dots indicate cells from samples at all respective time points; red dots indicate cells from selected time point and condition. Black and white arrowheads indicate presence and absence of populations, respectively, when comparing intact tail to 1 dpa samples. (**A**) A continuous change in the gene expression profile of goblet cells takes place during development both in regeneration-competent and -incompetent tails. (**B**) Cell state changes take place in motor neurons in response to amputation, both in regeneration-competent and -incompetent tails. (**C**) Differential gene expression changes take place in epidermis between regeneration-competent and -incompetent tails, identifying a cell state change specific to regeneration.

Fig. 3. Regeneration-organizing cells (ROCs) characterize the specialized wound epidermis in regeneration-competent tadpoles. (**A**) ROCs express high *Lef1* mRNA levels and reappear after amputation specifically in regeneration-competent tadpoles. Gray dots indicate *TP63*-positive epidermal clusters; dots with a black outline indicate selected sample. Relative *Lef1* expression is visualized for each cell. (**B**) ROCs (TP63+/LEF1+ cells, denoted by asterisks) are localized along the midline edge of the epidermis in intact tails. Green, pbin7Lef; red, TP63. Scale bar: 500 μm. (**C**) ROCs (LEF1+) remain along the posterior trunk after amputation (asterisks) but are removed from the amputation plane (empty arrowheads). ROCs specifically reappear in the amputation plane of 1 dpa regeneration-competent tadpoles (white arrowhead). hpa, hours post-amputation. Green, pbin7Lef:GFP. Scale bars: 250 μm. A total of ≥3 tadpoles per condition were imaged from two biological replicates. (**D**) Quantification of TP63+/LEF1+ cells at the amputation plane (mean ± standard deviation) shows a significant reduction in regeneration-incompetent tadpoles at 1 dpa (the total number of tadpoles assayed, n = 12 and 11 for competent and incompetent samples, respectively; both from two biological replicates). *P < 0.001.

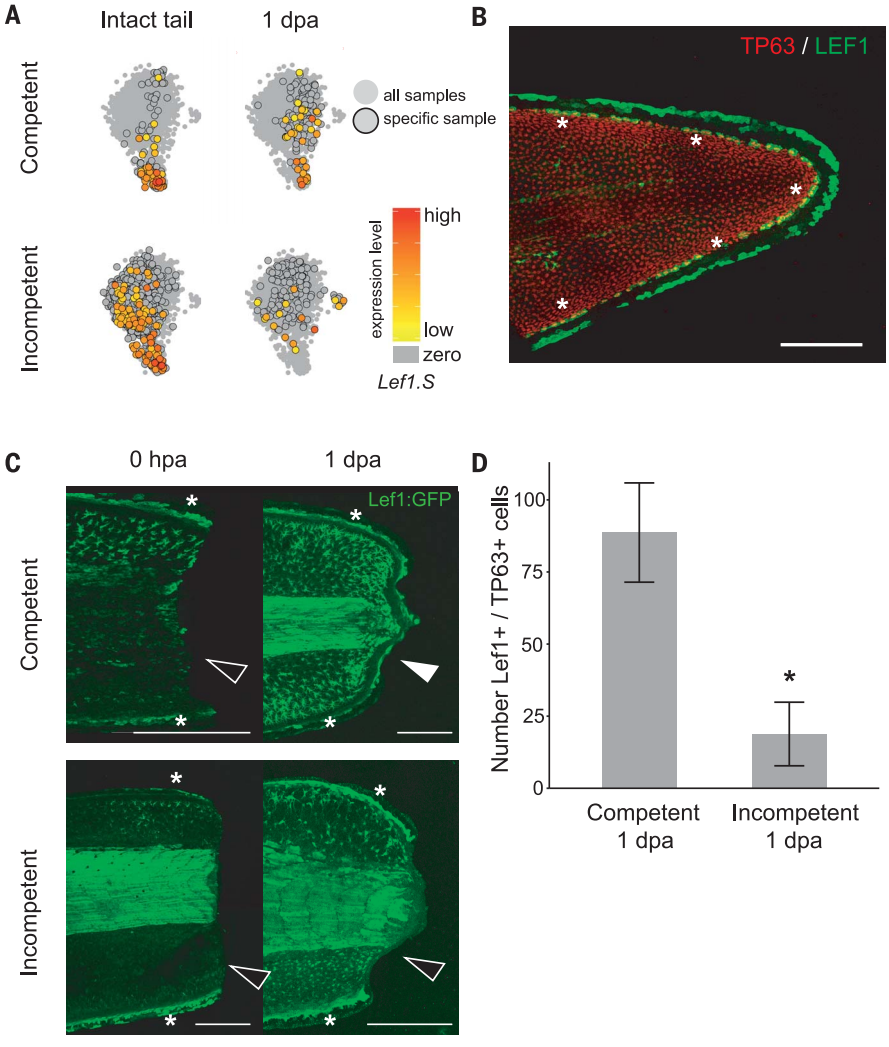

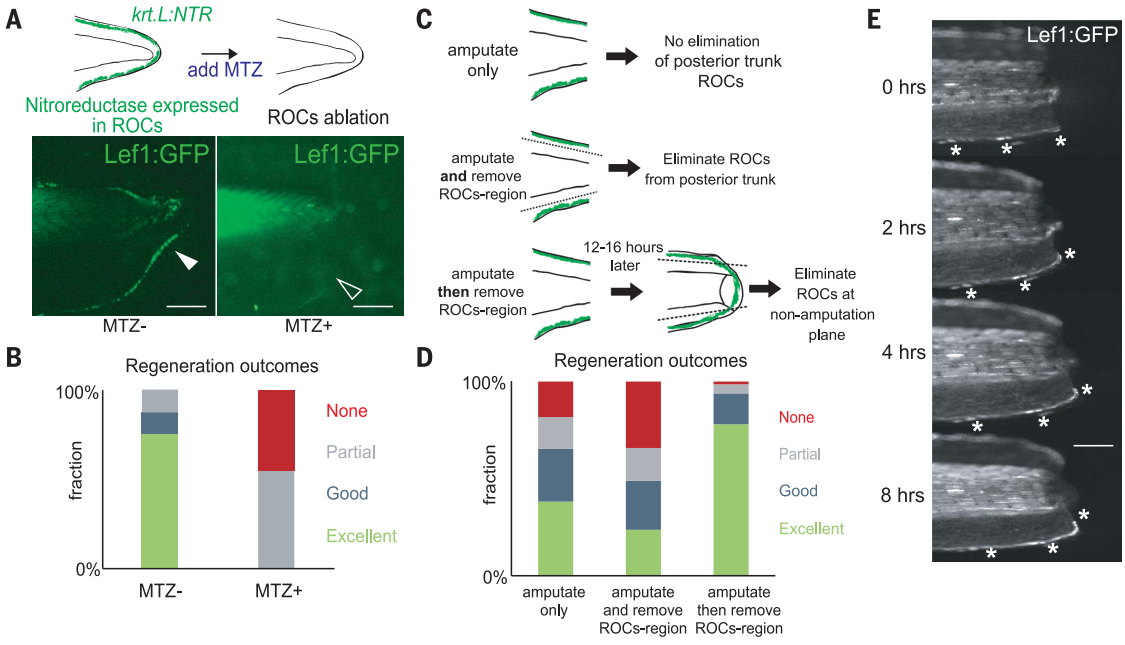

Fig. 4. Relocalization of ROCs to the amputation plane mediates tail regeneration. (**A**) NTR/MTZ–mediated ablation of ROCs during regeneration. pbin7Lef:GFP/Krt.L:NTR F_0 transgenic tadpoles (bottom) show successful cell ablation at 3 dpa: GFP-positive ROCs are present in control (white arrowhead) but lost in MTZ-treated animal (empty arrowhead). Scale bars: 1 mm. (**B**) ROC-ablated tadpoles cannot regenerate (n = 11 from two biological replicates). (**C**) Schematic of ROCs-containing-region manual removal protocol. Green indicates localization of ROCs. (**D**) Manual removal of posterior trunk ROCs concurrent with tail amputation reduces regeneration (n = 45 from five biological replicates), but manual removal of posterior trunk ROCs 12 to 16 hpa does not negatively affect regeneration (n = 95 from three biological replicates). (**E**) Time-lapse images of ROCs relocating to the amputation plane, as assessed by pbin7Lef:GFP. Asterisks denote cells with brighter GFP that can be tracked (n = 8 from three biological replicates). Scale bar: 500 μm.

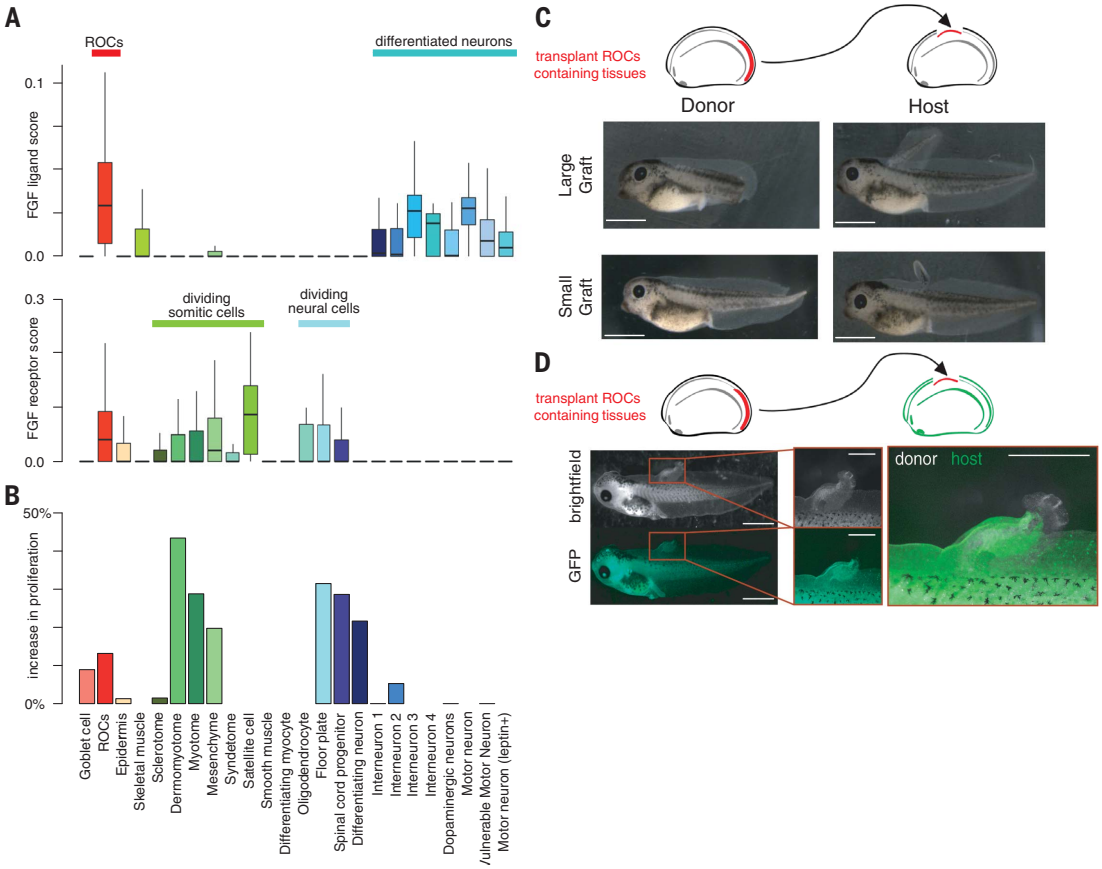

Fig. 5. ROCs act as a signaling center coordinating progenitor outgrowth during tail regeneration. (**A**) Expression of FGF ligands (top) and FGF receptor (bottom) shown for selected cell types as a boxplot (outliers are not shown). (**B**) Barplot indicating the change in the fraction of cells in G_2/M and S phases between regeneration-competent 2 dpa and regeneration-incompetent intact tail samples, all taken at 5 dpf. (**C**) (Left) Removal of large or small ROC-containing tissues causes tail development defects in donors (n = 20). (Right) Grafting these regions to the trunk enables tail-enriched or fin-enriched distal growth in hosts, respectively. Matching donor-acceptor pairs are shown 2 days postgrafting (n = 20 from three biological replicates). (**D**) Nonlabeled grafts to CMV:GFP positive embryos induce outgrowth containing GFP-positive cells; donor tissues are at the tip of the ectopic structure (n =12 from three biological replicates). Green, CMV:GFP. Scale bars: full tadpoles, 1 mm; zoomed grafts and merged graft images, 500 μm.

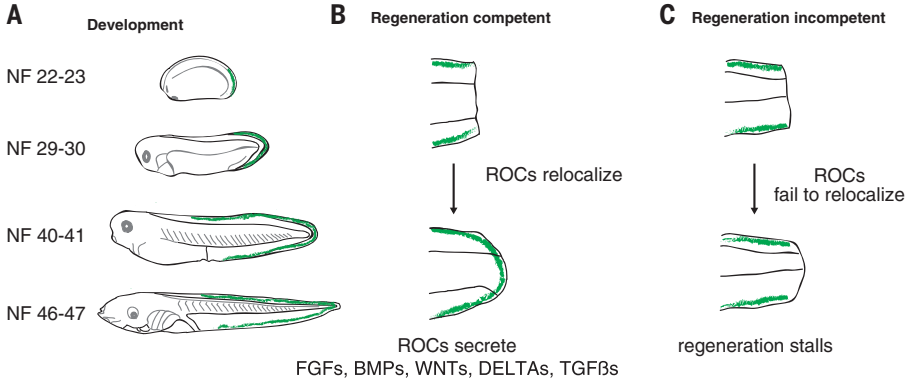

Fig. 6. ROC-based model of tail regeneration. (**A**) Transcriptional signature of ROCs first appears in NF stage 22 to 23 embryos at the tip of the tail bud, then it expands along the midline edge of the epidermis from the tail tip to the posterior trunk during development (table S2). (**B** and **C**) Relocalization of ROCs to the wound area forms the specialized wound epidermis and is a hallmark of successful tail regeneration.

Next, we asked whether inhibition of pathways that are necessary for wound epidermis formation, which are rapidly up-regulated after injury, interfere with the mobilization of ROCs to the amputation plane. Indeed, chemical inhibition of reactive oxygen species (ROS) production (*13*, *18*, *19*) or the transforming growth factor–β (TGFβ) pathway (*20*) resulted in significantly reduced ROC migration (fig. S8). In contrast, inhibition of the fibroblast growth factor (FGF) pathway, which is known to not affect wound epidermis formation (*15*), had no significant effect on ROC migration (fig. S8). Hence, wound-induced ROS production and TGFβ pathway activation are necessary for ROCs to migrate to the amputation plane, where they form the wound epidermis.

ROCs are a signaling center promoting proliferation

To understand the essential role played by ROCs during regeneration, we used our scRNA-seq data to dissect their transcriptional signature. Ligands of signaling pathways that are known to be required for regeneration and that increase proliferating cell numbers, such as FGF (*15*), BMP (*5*, *21*), WNT (*15*), NOTCH (*5*), and TGFβ (*20*), are simultaneously expressed in ROCs but not in any other cell type. In contrast, receptors for these pathways are mostly expressed in progenitor cell types (Fig. 5A and fig. S9). Moreover, we found that progenitor populations at the amputation site showed an increase in the fraction of cells in G_2/M and S phases during regeneration (Fig. 5B). These results suggest that ROCs function as a signaling center by secreting factors that promote progenitor proliferation in multiple tissues. Such an increase in proliferation can explain how tissue loss can be reconstituted from progenitors of the tail without requiring the emergence of a new multipotent cell state or states.

Having established the central role of ROCs during regeneration, we then asked whether they resemble other cell types associated with early development. ROCs express markers of limb development and appendage growth (fig. S10), including the limb apical ectodermal ridge (AER) regulating transcription factors *Sp8* and *Sp9* (*22*). The AER is a structure formed at limb-bud tips that plays an essential role in limb growth and patterning by sending extracellular signals to underlying tissues (*23*). In urodele limb regeneration, a similar structure, the apical epithelial cap (AEC), is shown to be necessary for limb regeneration (*1*). Although ROCs resemble AER and AEC transcriptionally (e.g., *Sp9*, *Msx2*, *Wnt5a*), we were not able to detect their well-known regulators [e.g., *Fgf2*, *Fgf4*, *Fgf8*, and *Cx43*(*Gja1*)] (fig. S10A). Despite this, we hypothesized that ROCs could play an instructive role during tail growth by secreting growth factors and extracellular cues in a manner similar to that of the AER during limb growth, and we aimed to test this using transplantation assays.

To isolate potential ROCs for grafting, we investigated where the transcriptional signature of ROCs is first detected during early embryonic development. Marker genes of ROCs first appear at the early tail-bud tip [Nieuwkoop and Faber (NF) stage 23] and later expand posteriorly along the midline edge of the epidermis (table S2). We grafted posterior tail-bud tissues of varying sizes, which contain ROCs, to the surface of different regions of trunk of a host embryo (Fig. 5C). All grafts induced ectopic outgrowth, regardless of graft size or implantation location. Larger grafts induced taillike structures, with a corresponding defect in donor tail growth; whereas smaller grafts, composed of only skin layers, induced finlike structures, with only a minor impact on the donor (Fig. 5C and fig. S11, A and B). In contrast, control grafts, in which dissected trunk skin tissues were transplanted, did not result in outgrowths and instead were incorporated into the host trunk (fig. S11C). To further pinpoint the cell type responsible for the outgrowths, we repeated our grafting experiments while simultaneously removing ROCs using the NTR/MTZ system. The ablation of *Krt.L*-expressing cells in the donor graft significantly reduced the length of the ectopic outgrowths (fig. S11, D and E), suggesting that ROCs are involved in the outgrowth phenomenon, although other cell types may also contribute.

If these distal growths are induced by the organizing abilities of the grafted ROCs, we would expect the transplanted cells to localize to the tip of the ectopic outgrowths. Indeed, when we tested this using GFP-labeled donor or host embryos, we found that most of the donor tissues were located at the tip of the ectopic structures. Moreover, host cells contributed to the ectopic structures in all grafts, indicating that ROCs can stimulate outgrowth of both donor and host cells (Fig. 5D and fig. S11, F and G). Together, these results suggest that ROCs act as an instructive signaling center that induces outgrowth during both the development and regeneration of the tail.

Outlook

Overall, our comprehensive analysis of cell types in the regenerating *Xenopus* tail provides a mechanistic understanding of the initiation and organization of tail regeneration via the reestablishment of a ROC-signaling center. By acting as the primary source of major growth factors and instructive signals, ROCs promote proliferation of underlying progenitors to regenerate tissue after amputation (Fig. 6). Our data also suggest that ROCs are a single cell type that characterizes the wound epidermis, a structure that is crucial for regeneration in many contexts (*2*). Investigation of other species (e.g., neonatal mouse, salamander) will indicate whether a ROC-based mechanism is a conserved feature of specialized wound epidermis formation and appendage regeneration.

Signatures of the specialized wound epidermis formation are absent in nonregenerating animals such as birds, adult mice, and adult frogs. However, reintroduction of molecules secreted from the specialized wound epidermis can reinitiate cell cycle entry to some degree in these animals (*24*–*26*). The discovery of a single cell type defining the wound epidermis offers a fresh perspective on cell replacement therapies, suggesting that "organizer grafts" may one day serve as an alternative to full organ replacement in regenerative therapies.

REFERENCES AND NOTES

1. E. M. Tanaka, *Cell* **165**, 1598–1608 (2016).
2. C. L. Stoick-Cooper, R. T. Moon, G. Weidinger, *Genes Dev.* **21**, 1292–1315 (2007).
3. C.-H. Chen, K. D. Poss, *Annu. Rev. Genet.* **51**, 63–82 (2017).
4. J. Li, S. Zhang, E. Amaya, *Regeneration* **3**, 198–208 (2016).
5. C. W. Beck, B. Christen, J. M. W. Slack, *Dev. Cell* **5**, 429–439 (2003).
6. L. McInnes, J. Healy, J. Melville, UMAP: Uniform Manifold Approximation and Projection for Dimension Reduction. arXiv:1802.03426 [stat.ML] (9 February 2018).
7. C. Gargioli, J. M. W. Slack, *Development* **131**, 2669–2679 (2004).
8. J. Chen *et al.*, *Cell Death Dis.* **8**, e3090 (2017).
9. J. Kang *et al.*, *Nature* **532**, 201–206 (2016).
10. N. R. Love *et al.*, *BMC Dev. Biol.* **11**, 70 (2011).

11. T. Sugiura, A. Tazaki, N. Ueno, K. Watanabe, M. Mochii, *Mech. Dev.* **126**, 56–67 (2009).
12. Y. Taniguchi, T. Sugiura, A. Tazaki, K. Watanabe, M. Mochii, *Dev. Growth Differ.* **50**, 109–120 (2008).
13. N. R. Love *et al*., *Nat. Cell Biol.* **15**, 222–228 (2013).
14. H. T. Tran, B. Sekkali, G. Van Imschoot, S. Janssens, K. Vleminckx, *Proc. Natl. Acad. Sci. U.S.A.* **107**, 16160–16165 (2010).
15. G. Lin, J. M. W. Slack, *Dev. Biol.* **316**, 323–335 (2008).
16. A. Tazaki *et al*., *Dev. Dyn.* **233**, 1394–1404 (2005).
17. R. I. Martinez-De Luna, M. E. Zuber, *Cold Spring Harb. Protoc.* **2018**, t100974 (2018).
18. F. Ferreira, G. Luxardi, B. Reid, M. Zhao, *Development* **143**, 4582–4594 (2016).
19. F. Ferreira, V. Raghunathan, G. Luxardi, K. Zhu, M. Zhao, *Nat. Commun.* **9**, 4296 (2018).
20. D. M. Ho, M. Whitman, *Dev. Biol.* **315**, 203–216 (2008).
21. C. W. Beck, B. Christen, D. Barker, J. M. W. Slack, *Mech. Dev.* **123**, 674–688 (2006).
22. Y. Kawakami *et al*., *Development* **131**, 4763–4774 (2004).
23. F. Petit, K. E. Sears, N. Ahituv, *Nat. Rev. Genet.* **18**, 245–258 (2017).
24. K. Kostakopoulou, A. Vogel, P. Brickell, C. Tickle, *Mech. Dev.* **55**, 119–131 (1996).
25. L. Yu *et al*., *Development* **137**, 551–559 (2010).
26. G. Lin, Y. Chen, J. M. W. Slack, *Dev. Cell* **24**, 41–51 (2013).

ACKNOWLEDGMENTS

We thank the Cambridge Institute Genomics Core for their support with this work on the 10X-Genomics and sequencing library preparations. The transgenic testes used in this study and pTransgenesis vectors were obtained from the European *Xenopus* Resource Centre, curated with funding from the Wellcome Trust/BBSRC, and maintained by the University of Portsmouth, School of Biological Sciences. Anti-PCNA and anti-PHH3 antibodies were provided by the Brand Lab. CFP-NTR construct was provided by J. Mumm and M. Zuber. We thank H. Ma and M. Huch for use of their stereoscopes. We thank A. Lun for advice on scRNA-seq analysis; J. Griffiths for assisting with the creation of the website; C. Baker and M. Minarik for their help during the revision period; B. Steventon, J. Robert, J. Kaufman, N. McGovern, and D. Wagner for general discussion of the single-cell data. We thank A. Philpott, V. Gaggioli, and E. Rawlins for their critical reading of the manuscript. **Funding:** C.A. is funded by University of Cambridge and Cambridge Trust. J.J. and J.B.G. are funded by a grant from the Wellcome Trust (101050/Z/13/Z). T.W.H., J.C.M., and B.D.S. are funded as part of a Wellcome Strategic Award to study cell fate decisions (105031/D/14/Z). T.W.H. is also supported by an EMBO Long-Term Fellowship (ALTF 606-2018). B.D.S. also acknowledges funding from the Royal Society E.P. Abraham Research Professorship (RP\R1\180165) and Wellcome Trust (098357/Z/12/Z). J.C.M. acknowledges core funding from the European Molecular Biology Laboratory and Cancer Research UK (A17197). This work is funded by a grant from the Wellcome Trust (101050/Z/13/Z) and supported by the Gurdon Institute core grant from Cancer Research UK (C6946/A14492) and the Wellcome Trust (092096/Z/10/Z). **Author contributions:** Conceptualization: C.A. and J.J.; Experiments: C.A. with assistance from J.J. with grafting; Computational analysis: T.W.H.; Data interpretation: C.A., T.W.H., and J.J.; Writing – original draft: C.A., T.W.H., and J.J.; Writing – review & editing: all authors; Supervision: J.C.M., B.D.S., and J.B.G. contributed to general supervision, and J.J. mainly supervised the project. **Competing interests:** The authors declare no competing interests. **Data and materials availability:** Sequencing data and processed gene counts are available on ArrayExpress with the accession number E-MTAB-7716. Analysis scripts are available at https://github.com/MarioniLab/XenopusTailRegeneration2019. Requests for materials and code should be addressed to J.J. and B.D.S.

SUPPLEMENTARY MATERIALS

science.sciencemag.org/content/364/6441/653/suppl/DC1
Materials and Methods
Figs. S1 to S11
Tables S1 to S3
References (*27–42*)

8 November 2018; accepted 17 April 2019
10.1126/science.aav9996